EVS26
Los Angeles, California, May 6-9, 2012

Electrochemical Performance of $LiFe_{0.99}La_{0.01}PO_4$ Coated with Different Organic Acids

George Ting-Kuo Fey[1*], Bo-Fu Chang[1], Kai-Pin Huang[1], Yi-Chuan Lin[1], Yung-Da Cho[1]
Hsien-Ming Kao[2], and Shih-Hung Chan[3]
[1]*Department of Chemical and Materials Engineering, National Central University, Chung-Li, Taiwan 32054, R.O.C*
***** *gfey@cc.ncu.edu.tw*
[2]*Department of Chemistry, National Central University, Chung-Li, Taiwan 32054, R.O.C*
[3]*Fuel Cell Center, Yuan Ze University, No.135, Yuandong Rd., Chung-Li, Taiwan 32073, R.O.C.*

Abstract

Olivine-type $LiFePO_4$ is one of the most popular cathode materials for high power Li-ion batteries. However, its intrinsic properties of poor conductivity and low lithium-ion diffusion limit its practical applications. In order to improve these disadvantages, we prepared the $LiFe_{0.99}La_{0.01}PO_4$/C composite materials by a solid state reaction method using La-ion as a metal dopant and organic diacids as carbon coating sources. In this work, the composite materials were characterized by XRD, DSC, SEM/mapping, TEM/EDS/SAED, and total organic carbon (TOC). Further, their electrochemical performance was examined. The conductivity results of the doped composites showed a distinct enhancement from 3.97×10^{-8} to 2.60×10^{-5} S cm^{-1}. The $LiFe_{0.99}La_{0.01}PO_4$/C composites using malonic and sebasic acids as carbon sources displayed an initial discharge capacity of 151 and 145 mAh g^{-1}, respectively, between 2.8 and 4.0 V at a 0.2 C rate. This is a significant improvement compared to the initial discharge capacity of 100 mAh g^{-1} of the un-doped bare $LiFePO_4$ sample, and it may be related to electronic conductivity enhancement by carbon coating and charge transfer kinetics improvement by La-ion doping.

Keywords: lithium battery, battery charge, energy storage

1 Introduction

Nowadays, rechargeable Li-ion cells are important components of portable devices, such as notebooks, entertainment and, telecommunication equipment . With the growth in applications worldwide, the science of battery technology is studied to take advantage of a growing market [1].

Lithium-ion batteries have been widely used in various devices due to the high energy density and excellent cyclic performance [2, 3]. To date, layered lithium cobalt oxide is still the main cathode used in commercial lithium-ion batteries [4]. The other Li-ion cathodes, such as lithium nickel oxide [5], lithium manganese oxide [6], and lithium iron phosphate also have been widely studied for various applications. However, most of the cathodes have shown structural instability, high material costs and significant capacity fading during cycling [7-9]. Lithium iron phosphate ($LiFePO_4$), since they were first proposed by Goodenough's group in 1997 [10], has been a popular cathode material because it is highly safe [11,12], low cost [10], environmentally benign [10], long cycle life[12], and has a flat

charge/discharge plateau (at 3.5 V) [13] and moderate theoretical capacity (170 mAh g^{-1}).
Despite the intrinsically poor electronic conductivity and lithium ion diffusion coefficient of pristine $LiFePO_4$, the electrochemical performance can be significantly improved by carbon coating [7] particle size optimizing [14], and transition metal doping [15, 16]. The above mentioned methods have been achieved by a solid-state reaction [17, 18], co-precipitation reaction [19], hydrothermal synthesis [20], solution synthesis [21], and sol-gel method [22].
In this work, we combined both metal doping and carbon coating methods to synthesize $LiFe_{0.99}La_{0.01}PO_4/C$ composite materials. Through our work, we have significantly improved the cell performance of $LiFePO_4$.

2 Experimental

$LiFe_{0.99}La_{0.01}PO_4/C$ composites were synthesized by a solid state reaction. The precursors were prepared by stoichiometric amounts of the reactants of Li_2CO_3 (99 wt.%, Aldrich), $FeC_2O_4{\bullet}2H_2O$ (98.5 wt.%, Aldrich), $NH_4H_2PO_4$ (98.5 wt.%, Aldrich) and $La(NO_3)_3{\bullet}6H_2O$ (99 wt.%, Aldrich). The above materials were mixed by ball-milling for 3 h. The mixtures were pre-heated in a tube furnace with a flowing Ar/H_2 mixture (95:5, v/v) at 320 ℃ for 12 h. After cooling down to room temperature, the precursors were grounded with malonic acid and/or sebasic acid in acetone for 30 min. The mixed precursors were pressed into pellets and annealed at 600 ℃ for 12 h under a Ar/H_2(95:5, v/v) atmosphere.
The cathodes are prepared by mixing a 85 wt.% active material, 10 wt.% conductive carbon black, and 5 wt.% poly(vinylidene fluoride) and binding in N-methyl-2-pyrrolidone (NMP) to form a homogeneous slurry. The slurry was coated on aluminum foil and dried at 383 K for 3 h in an oven. Meanwhile, the dry mixtures were cut into the needed size. We used the lithium foil as a counter electrode, Celguard 2400 microporous polypropylene membrane as separator, then took ethylene carbonate : diethyl carbonate (EC:DEC) (Tomiyama Chemicals) in the volume ratio 1:1 with 1M $LiPF_6$ as the electrolyte. Finally, the coin cells were assembled in a glove box within argon atomosphere. All the cycling tests were measured at a current of 0.2 C with cut-off voltages of 2.8-4.0 V (versus Li/Li^+) at 25 °C in multi-channel battery taster (Maccor 4000).
$LiFe_{0.99}La_{0.01}PO_4$ samples were identified for the phase purity by X-ray diffractometer (XRD), Siemens D-5000, Mac Science MXP18, with a nickel-filtered Cu-K radiation source (λ = 1.5405 Å). The diffraction patterns were measured by X-ray diffractometer with Cu-Kα radiation identifying the crystalline phase of the materials at a scan rate of 4°/min between 15° to 80°. The morphology of the $LiFe_{0.99}La_{0.01}PO_4/C$ composite materials were observed by scanning electron microscope (SEM; Hitachi S-3500 V) and analyzed atomics element by energy dispersive spectroscopy (EDS) with Link Isis apparatus (Oxford). The microstructure, lattice phase and carbon coating thickness were observed by high resolution transmission electron microscope (HRTEM, Hitachi HF 2000) equipped with a LaB_6 gun. Furthermore, electron diffraction patterns and cathode materials composition were measured by selected area electron diffraction (SAED) and nanobeam energy dispersion X-ray (EDX).
The carbon content investigation was measured by an OIA Model Solids module for the total organic carbon (TOC) with an oxygen gas rate of 40 kgf cm^{-2}. The Raman spectra were recorded by ISA T64000 double beam pass spectrometer provided with a microscope stage for examining samples which was applying 180◦ incident geometry. The physical argon-ion laser was used for exciting laser Raman spectra with a 515 nm laser beam at an incident power of ca. 10 mW. The scanning rate was 10 cm^{-1} min^{-1} for measuring the spectra.
CV experiments were carried out by slow scan cyclic voltammetry with three-electrode glass cell in order to determine the phase transitions. The experiments were performed by using the lithium metal foil as the counter and reference electrodes, and put into electrolyte which we mention above while assembling cells. The linear potential sweep patterns were performed by Solartron 1287 Electrochemical Interface with the scanning rate of 0.1 mVs^{-1} between 2.8 and 4.0 V. The particle size was measured by a dynamic light-scattering particle size analyzer (Malvern Zetasizer Nano).

3 Results and Discussion

3.1. Concentration of La-ion doping

The specific capacity vs. number of discharge cycles were shown in Fig. 1. It is obvious the 1 mol% La-doped $LiFePO_4/C$ materials show the greatest performance with malonic acid (1^{st} D.C.=151 mAh g^{-1}) or sebasic acid (1^{st} D.C.= 145 mAh g^{-1}) as the carbon source due to the improvement of conductivity, as shown in Table 1. The samples with other doping concentrations

Table 1: Comparison of conductivity, carbon content, and I_D/I_G ratios of La-doped samples.

Term	Conductivity (S cm^{-1})	TOC (wt.%)	Raman Peak (cm^{-1})		Raman Area (a.u.)	I_D/I_G ratio	Capacity (mAh g^{-1})	Condition
Carbon-free	3.97E-07	0.13					104	
50 wt.% Malonic Acid	9.80E-06	0.96	sp2	1341 (D band)	124,172	4.60	148	1.0 mole% La 873 K 12 h
				1604 (G band)	26,981			
			sp3	1020	132,732			
				1525	31,235			
60 wt.% Malonic Acid	2.60E-05	1.65	sp2	1335 (D band)	21,143	4.52	151	
				1567 (G band)	4,677			
			sp3	1250	20,831			
				1503	4,874			
70 wt.% Malonic Acid	8.27E-06	2.10	sp2	1333 (D band)	21,590	4.76	146	
				1590 (G band)	4,536			
			sp3	1320	26,859			
				1530	4,313			
34 wt.% Sebasic Acid	3.17E-05	4.03	sp2	1326 (D band)	151,708	4.90	142	1.0 mole% La 873 K 12 h
				1592 (G band)	30,974			
			sp3	1162	180,917			
				1517	18,317			
36 wt.% Sebasic Acid	2.25E-05	4.69	sp2	1342 (D band)	138,910	4.66	145	
				1593 (G band)	29,809			
			sp3	1248	117,392			
				1509	27,885			
38 wt.% Sebasic Acid	2.13E-05	4.99	sp2	1336 (D band)	98,376	4.70	140	
				1594 (G band)	20,931			
			sp3	1236	116,272			
				1518	4,757			

present slightly capacity decay after cycling, which is similar to the results of Co-ion doping [23]. Although the conductivity is proportional to the amount of La-doping, the over amount of La-ion doping might cause the lattice distortion of $LiFePO_4/C$, which would inhibit the Li^+ diffusion during the charge/discharge process [24].

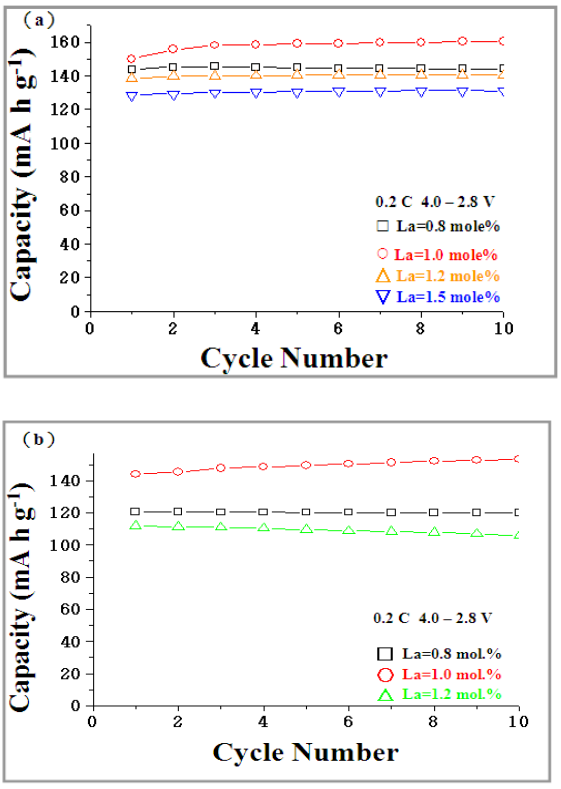

Figure 1: The synthesis of La-ion doping amount effects on $LiFePO_4$ for (a) malonic acidand (b) sebasic acid.

3.2. Amount of carbon sources

The discharge profiles of $LiFe_{0.99}La_{0.01}PO_4/C$ composites prepared at 873 K for 12 h and coated with various weight percents of malonic and sebasic acids are displayed in Fig. 2. Based on the discharge capacity at 50 cycles at a 0.2 C-rate between 4.0-2.8 V, the best coating level was 60 wt.% for malonic acid, which had a discharge capacity of 160 mAh g^{-1} as shown in Fig. 2(a). On the other hand, the best coating level was 36 wt.% for sebasic acid, which had a discharge capacity of 144 mAh g^{-1} as shown in Fig. 2(b).

Carbon coating can effectively inhibit of particle size [25], as confirmed in Table 2. Small particle size allows easy penetration of the electrolyte and provides a short pathway for Li^+ diffusion in the active material crystals. The first-cycle discharge capacity of the bare $LiFePO_4$ sample was near 100 mAh g^{-1}, while the 50, 60 and 70 wt.% malonic acid-coated samples had first-cycle discharge capacities of 148, 150 and 146 mAh g^{-1}, respectively. After the first cycle, the discharge capacity of 60 wt.% malonic acid-coated samples increased from 150 to 160 mAh g^{-1} and remained steadily even after 100 cycles. As shown in Fig. 1(b), the 32, 34, 36, and 38 wt.% sebasic acid-coated samples had first-cycle discharge capacities of 128, 141, 144, and 141 mAh g^{-1}, respectively. The capacity decreased more at higher coating levels because of the presence of inactive residual carbon in the electrode, adversely affecting charging and discharging efficiencies [25, 26].

Table 2: Conductivity, carbon content, specific capacity and particle size of $LiFe_{1-x}La_xPO_4/C$ samples synthesized with (a) malonic acid and (b) sebasic acid.

(a)

Term	Conductivity (S cm^{-1})	TOC (wt.%)	Capacity (mAh g^{-1})	Particle Size (nm)	Condition
Bare	3.97E-07	0.13	100	764	Carbon-free/ $LiFe_{0.99}La_{0.01}PO_4$
0.8 mole% La	9.37E-06	1.52	141	286	60 wt.% Malonic Acid
1.0 mole% La	2.60E-05	1.65	151	387	873 K
1.2 mole% La	4.66E-05	1.46	138	334	12 h
1.5 mole% La	8.23E-05	1.70	125	337	
50 wt.% Malonic Acid	9.80E-06	0.96	148	288	1.0 mole% La
60 wt.% Malonic Acid	2.60E-05	1.65	151	387	873 K
70 wt.% Malonic Acid	8.27E-06	2.10	146	485	12 h
823 K	1.64E-05	1.10	138	304	1.0 mole% La
873 K	2.60E-05	1.65	151	387	60 wt.% Malonic Acid
923 K	8.98E-06	2.20	126	495	12 h
8 h	6.17E-07	1.33	138	291	1.0 mole% La
12 h	2.60E-05	1.65	151	387	873 K
16 h	3.76E-07	1.92	135	616	60 wt.% Malonic Acid

(b)

Term	Conductivity (S cm^{-1})	TOC (wt.%)	Capacity (mAh g^{-1})	Particle Size (nm)	Condition
Bare	3.97E-07	0.13	100	764	Carbon-free/ $LiFe_{0.99}La_{0.01}PO_4$
0.8 mole%	1.32E-05	4.37	123	474	36 wt.% Sebasic Acid
1.0 mole%	2.25E-05	4.69	145	484	873 K
1.2 mole%	5.01E-05	4.44	127	486	12 h
32 wt.% Sebasic Acid	1.58E-05	3.99	138	347	1.0 mole% La 873 K 12 h
34 wt.% Sebasic Acid	3.17E-05	4.03	142	480	
36 wt.% Sebasic Acid	2.25E-05	4.69	145	484	
38 wt.% Sebasic Acid	2.13E-05	4.99	140	757	
823 K	1.98E-05	4.53	118	456	1.0 mole% La
873 K	2.25E-05	4.69	145	484	36 wt.% Sebasic Acid
923 K	3.14E-05	4.88	131	527	12 h
8 h	1.52E-05	4.45	144	290	1.0 mole% La
12 h	2.25E-05	4.69	145	484	873 K
16 h	9.87E-06	4.13	136	637	36 wt.% Sebasic Acid

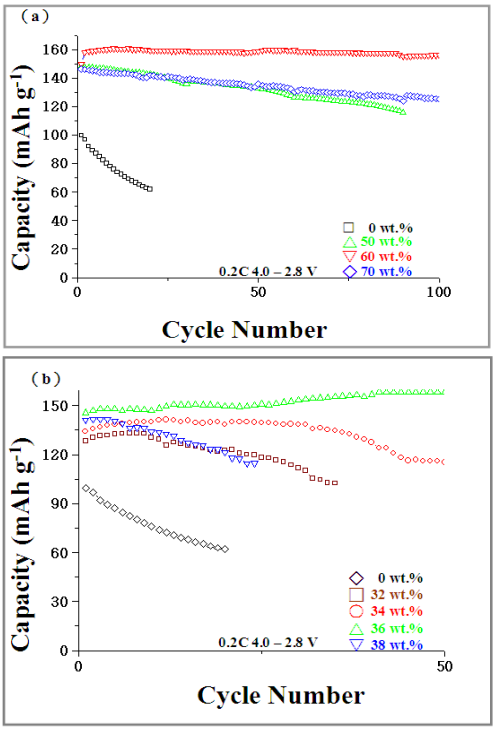

Figure 2: Discharge capacity vs. cycle number for pure $LiFePO_4$ and 1 mol.% La-doped materials treated with various wt.% (a) malonic acids and (b) sebasic acids.

3.3. Synthesis temperature

Fig. 3 shows the cyclic discharge performance of $LiFe_{0.99}La_{0.01}PO_4/C$ synthesized at 823, 873 and 923 K. The samples synthesized at 873 K with malonic acid and sebasic acid deliver the best initial discharge capacities of 151 and 145 mAh/g, respectively. It was known $LiFePO_4$ particles agglomerate under a high temperature environment, which might lead to large particle size, as confirmed in Table 2. However, lower temperature might result in poor crystalline structure. As a result, too high or too low temperatures are not beneficial to the cell performance of La-doped $LiFePO_4/C$ composites [11, 26, 27]. Yamada et al. reported an obvious growth in particle size when the sintering temperature rose above 873K [11], which is similar to what happened in our study.

3.4. X-ray diffraction

Fig. 4 shows the XRD profiles of bare and different carbon coated $LiFe_{0.99}La_{0.01}PO_4$ prepared at 873 K for 12 h. All diffraction lines are indexed to the orthorhombic Pnma space group (JCPDS card no. 40-1499), indicating La-ion doping did not affect the structure of the samples. According

to the Scherrer's law, The crystallite size (D) cab be calculated from the follow equation:

$$\beta\cos(\theta)=k\lambda/D \quad (1)$$

where B is the full-width-at-half-maximum (FWHM) of the XRD peak (1 1 1) and k is a constant (0.91). The calculated crystalline sizes of La-doped $LiFePO_4$/C composites with free carbon, 60 wt.% malonic acid and 36 wt.% sebasic acid were 27.6, 25.4 and 25.6 nm, respectively. It was reported that the particle size of $LiFePO_4$ materials could be restrained by the carbon coating method [29].

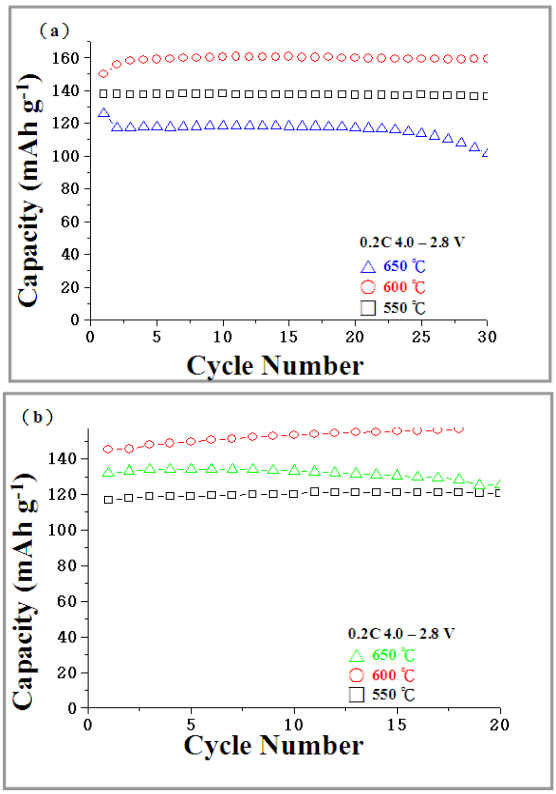

Figure 3: Discharge capacity vs. cycle number for 1 mol% La-doped $LiFePO_4$/C composites synthesized at 550, 600, and 650 ℃ with (a) malonic acid; (b) sebasic acid.

3.5. TOC and Conductivity analysis

The total organic carbon (TOC) and electronic conductivity of $LiFe_{0.99}La_{0.01}PO_4$/C synthesized at various conditions are presented in Table 2. All La-doped samples show better electronic conductivity than the bare one because the doping method could assist with charge transferring and enhance electric conductivity [30]. It was shown that the conductivity is roughly proportional to the amount of La-doping, but the over amount of La-ion doping might cause a lattice distortion of $LiFePO_4$/C, which would lead to a lower discharge capacity.

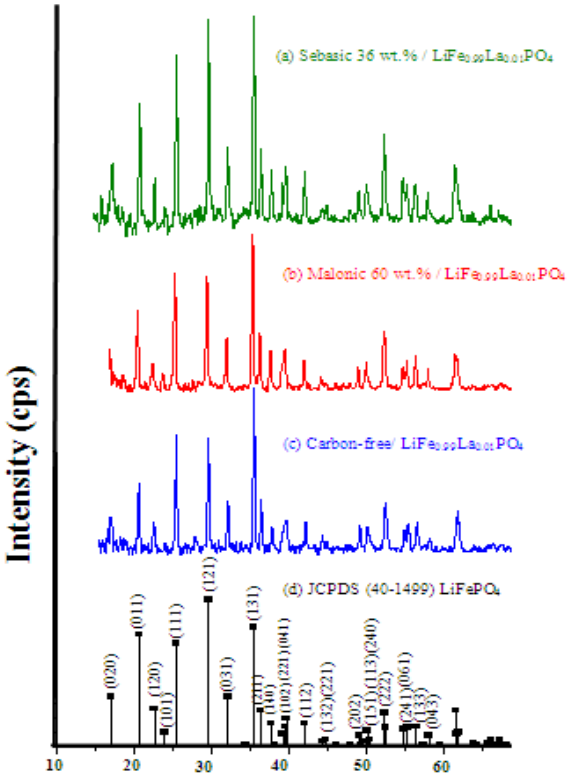

Figure 4: X-ray powder diffraction patterns of $LiFe_{0.99}La_{0.01}PO_4$/C composites with (a) Sebasic acid 36 wt.%；(b) Malonic acid 60 wt.%；(c) Carbon-free ；(d) JCPDS(40-1499).

The TOC results indicated that the residual carbon content in cathodes increased as increasing amounts of carbon source were added. However, there was no direct relationship between the electrochemical performance of cathode materials and electronic conductivity or residual carbon amounts. It demonstrated that the electrochemical performance is a complex function affected by more factors, such as the particle size of the active material, the thickness of the carbon coating layer, the kind of conductive carbon network, and the surface area of the carbon precursor.

3.6. Morphology

The morphology of the $LiFe_{0.99}La_{0.01}PO_4$/C synthesized with malonic acid and sebasic acid was studied by SEM and TEM/EDS images, as shown in Fig. 5 to Fig. 8. The SEM images (Fig. 5 and 6) show that numerous nano-sized particles aggregate to form micron sized clusters. Each element (C, Fe, and La) has a similar contour in the element mapping analysis, verifying a uniform

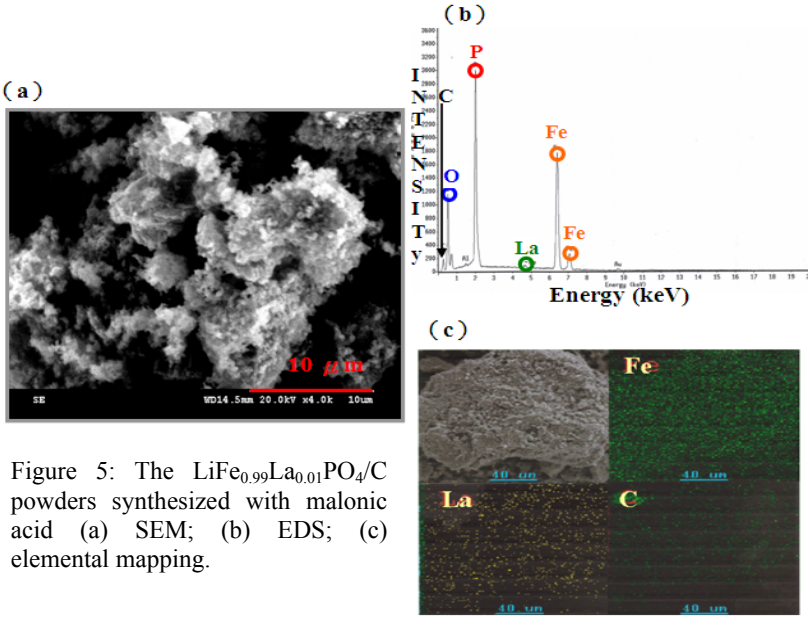

Figure 5: The $LiFe_{0.99}La_{0.01}PO_4/C$ powders synthesized with malonic acid (a) SEM; (b) EDS; (c) elemental mapping.

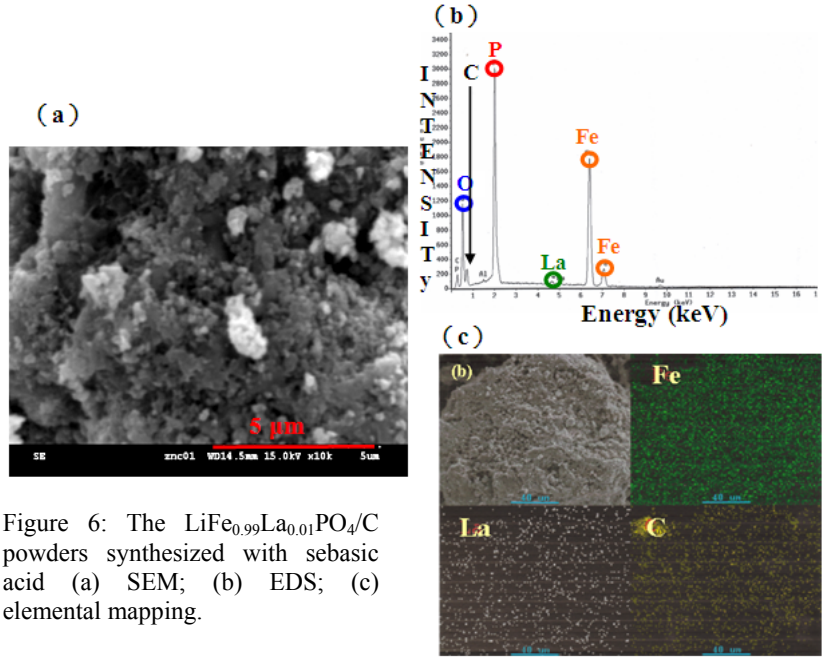

Figure 6: The $LiFe_{0.99}La_{0.01}PO_4/C$ powders synthesized with sebasic acid (a) SEM; (b) EDS; (c) elemental mapping.

distribution and homogeneous existence of La ion dopant in $LiFePO_4$ crystal.

In Fig. 7 and Fig. 8, the EDS analyses in Fig. 7(d) and Fig. 8(d) confirmed that the dark areas include Fe, P, O, C and La components, and the grayish area has only a C peak. The SAED analysis images of grayish layer show a halo ring, which confirmed a presence of amorphous carbon. The dark region shows a distinct lattice image, indicating a well-crystallized $LiFePO_4/C$ structure [32]. The grain sizes of our both samples were around 25~30 nm, which was consistent with the XRD analysis. We could observe the samples coated with 3~6 nm thick carbon layers. R. Dominko et al. [31] reported the thinner carbon layer is a key to higher specific discharge capacity.

3.7. Cyclic voltammetry

Fig. 9 and 10 show the cyclic voltammetry（CV）of $LiFe_{0.99}La_{0.01}PO_4/C$ materials synthesized with malonic acid and sebasic acid. Only a pair of anodic and cathodic peaks was observed due to the Fe^{2+}/Fe^{3+} redox reaction accompanying Li^+ insertion and extraction. The anodic peak at ~3.54 V represents the oxidation of Fe^{2+} to Fe^{3+}, while the cathodic peak at ~ 3.30 V is due to the reduction of Fe^{3+} to Fe^{2+}. The symmetrical sharp redox peaks imply that kinetics of the lithium diffusion is fast in the $LiFe_{0.99}La_{0.01}PO_4/C$ structure

Figure 7: $LiFe_{0.99}La_{0.01}PO_4/C$ synthesized with malonic acid: (a)(b)(c)TEM micrographs ; (d)(e) SAED and EDS patterns.

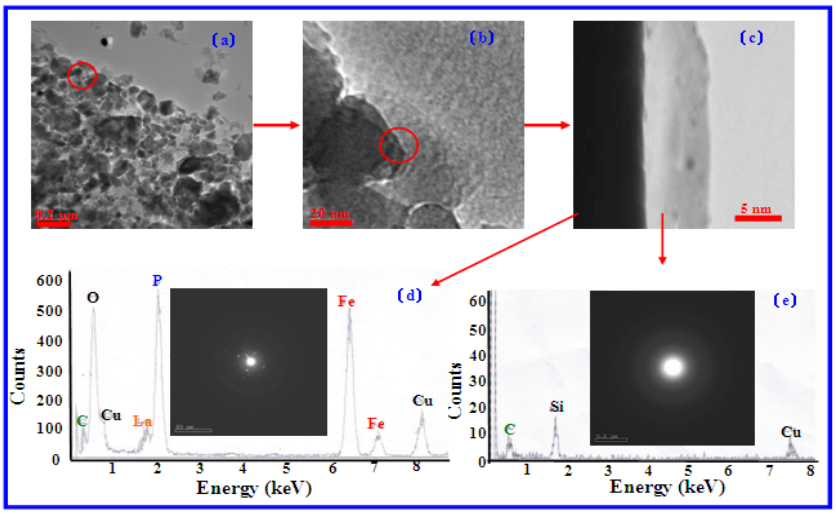

Figure 8: $LiFe_{0.99}La_{0.01}PO_4/C$ synthesized with sebasic acid: (a)(b)(c)TEM micrographs ; (d)(e) SAED and EDS patterns.

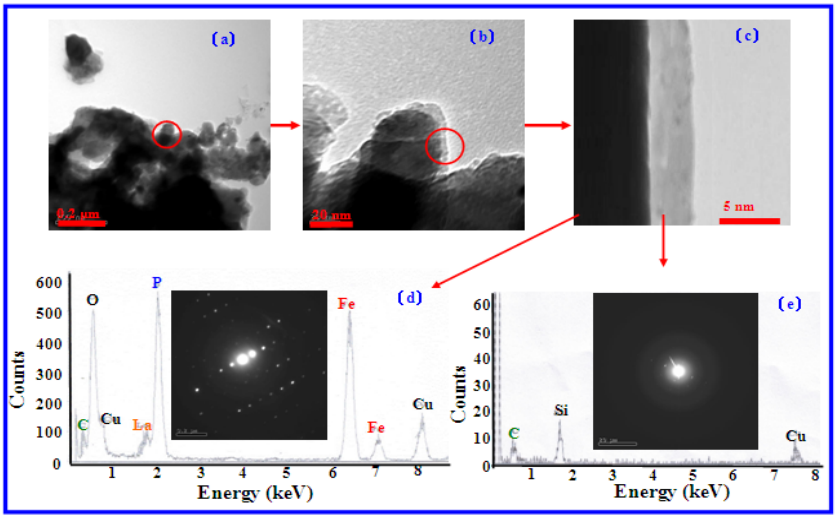

with better reversibility for lithium intercalation/ deintercalation. The voltage difference (ΔV) between the anodic and cathodic peaks is only 0.24 V, indicating less polarization of the $LiFe_{0.99}La_{0.01}PO_4/C$ materials.

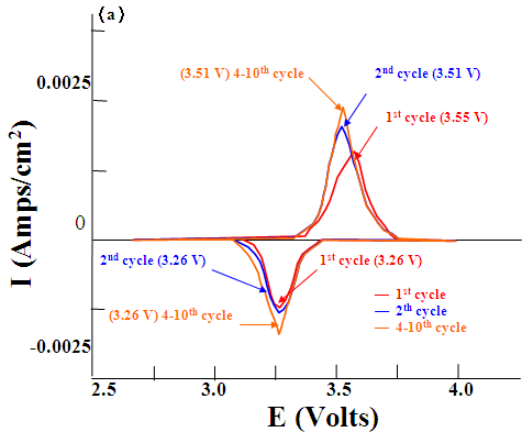

Figure 9: Cyclic voltammetry of $LiFe_{0.99}La_{0.01}PO_4$ synthesized with malonic acid as a carbon source.

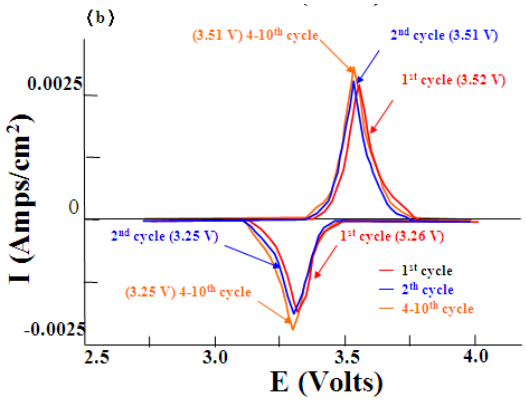

Figure 10: Cyclic voltammetry of $LiFe_{0.99}La_{0.01}PO_4$ synthesized with sebasic acid as a carbon source.

3.8. Raman spectroscopy

Fig. 11 and 12 were the Raman spectra of $LiFe_{0.99}La_{0.01}PO_4$ coated with different weight percents of malonic acid and sebasic acid. All Raman spectra show two intense and broad bands located at ~1350 and ~1590cm^{-1}, respectively,

which can be deconvoluted into four peaks at around 1190, 1350 (D band), 1518, and 1590 cm^{-1} (G band), and the results are shown in Table 1. The I_D/I_G ratio can be used to determine the degree of carbon disorder on the surface of the materials. A lower I_D/I_G ratio in Raman spectrum indicates more graphene clusters in the structure of carbon, which would enhance the electronic conductivity of the residual carbon. A slight peak located at 940 cm^{-1} was the intermolecular vibration of PO_4 called symmetric stretching mode (v1)[33], which might be a signal illustrating the uniform carbon coating over cathode materials[34].

From Table 1, the minimum I_D/I_G ratio occurred when 60% malonic acid was added, indicating more useful graphitized carbon became coated on the $LiFePO_4$.

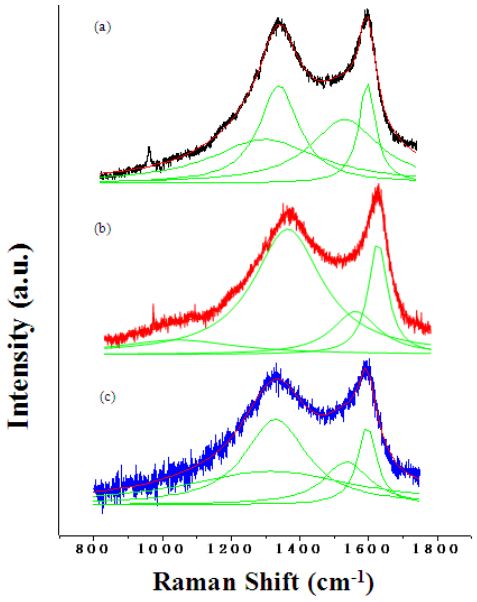

Figure 11: Raman spectra of the $LiFe0.9La_{0.1}PO_4/C$ composites synthesized with (a) 50%; (b) 60%; (c) 70% malonic acid.

3.9. Thermal stability studies

In order to study the thermal stability of $LiFe_{0.99}La_{0.01}PO_4/C$ composites under a delithiation condition, DSC analysis was carried out. Fig. 13 shows the DSC profiles of 4.5V charged bare $LiFePO_4$ and $LiFe_{0.99}La_{0.01}PO_4/C$ composites synthesized with 60% malonic acid and 36 wt.% sebasic acid. All exothermic heat flow was detected within a wide temperature range of 373–823 K. The total exothermic heat for the sample with malonic acid and sebasic acid as the carbon source was only 103.9 and 93.7 J g^{-1}, respectively, which is lower than the bare $LiFePO_4$ (109.4 J g^{-1}). Furthermore, the onset temperature of the La-doped sample is the lowest compared to bare $LiFePO_4$, $LiCoO_2$, $LiNi_{0.8}CoO_2$, and $LiMn_2O_4$ cathode materials [36]. The excellent thermal stability of the $LiFe_{0.9}La_{0.1}PO_4/C$ composites could make it commercially feasible for large battery applications, such as EVs.

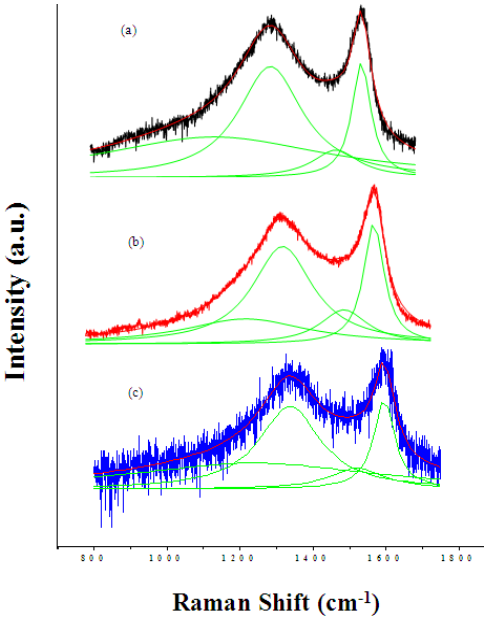

Figure 12: Raman spectra of the $LiFe_{0.9}La_{0.1}PO_4/C$ composites synthesized with (a) 34%; (b) 36%; (c) 38% sebasic acid.

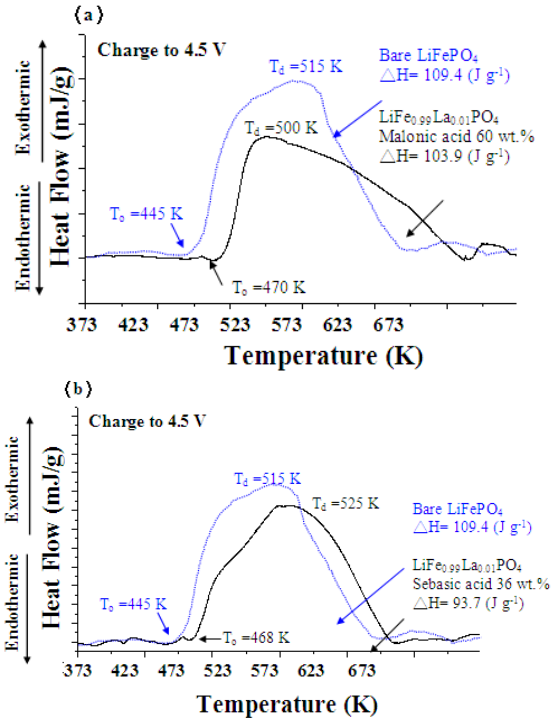

Figure 13: DSC profiles of La-doped $LiFePO_4$/ C(a) malonic acid; (b) sebasic acid. Charged to 4.5 V.

3.10. Rate and high temperature performance

Because high current density would increase the charge/discharge polarization voltage which could mask the true rate capability of the material, we changed the charge/discharge cut-off voltage range from 4.0-2.8 V to 4.6-2.0 V, as shown in Fig. 14. It clearly demonstrates that Sb-doping and carbon coating can significantly improve the high rate performance of the material due to the enhanced electronic conductivity. Both samples treated with malonic acid or sebasic acid could sustain a 10 C-rate, and this rate capability is equivalent to charge or discharge in 6 min.

Fig. 15 shows the discharge capacity of the $LiFe_{0.9}La_{0.1}PO_4/C$ composites at 60 ℃. It can be seen that both the samples synthesized with malonic acid and sebasic acid presented cycling stability up to 10 cycles with an initial capacity of 159 and 150 mAh g^{-1}, respectively. These findings support the viability of these composites for EV or HEV battery applications.

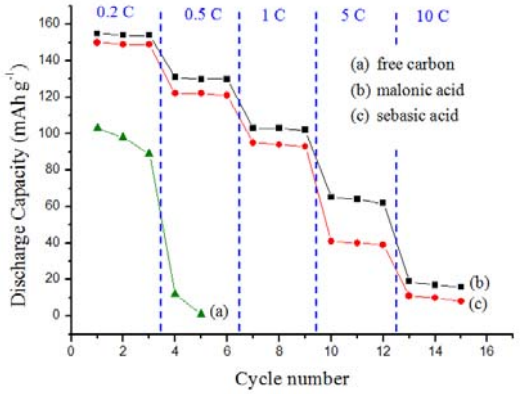

Figure 14: Rate performance of the $LiFe_{0.9}La_{0.1}PO_4/C$ composites synthesized with (a) free carbon; (b) 60% malonic acid; (c) 36% sebasic acid in the range of cut-off voltages: 4.6/2.0 V.

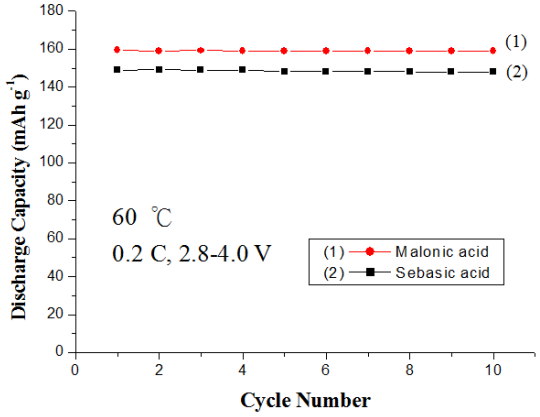

Figure 15: Discharge capacity vs. cycle number at 60 ℃ for the $LiFe_{0.9}La_{0.1}PO_4/C$ synthesized with malonic acid or sebasic acid.

4 Conclusions

We have successfully used a solid-state method to prepare $LiFe_{0.99}La_{0.01}PO_4/C$ cathode materials with malonic acid or sebasic acid as the carbon source. The X-ray diffractometer (XRD) results indicated that La-ion doping did not affect the structure of the samples. The thickness of carbon coating layer on the sample surface was about 3~6 nm, as confirmed by the TEM images. Electrochemical measurements showed the $LiFe_{0.99}La_{0.01}PO_4/C$ composites using malonic and sebasic acids as carbon sources displayed an initial discharge capacity of 151 and 145 mAh g^{-1}, respectively, between 2.8 and 4.0 V at a 0.2 C rate. The excellent cell performance might be contributed to the improvement of electronic conductivity from 3.97E-8 to 2.25E-5 S cm^{-1} by both La doping and carbon coating. Furthermore, the samples show an excellent thermal stability, which is suitable for large battery applications, such as EVs.

References

[1] J. M. Tarascon, M. Armand, *Issues and challenges facing rechargeable lithium batteries*, Nature, 414 (2001), 359-367.

[2] B. Scrosati, *Challenge of portable power*, Nature, 373 (1995), 557-558.

[3] R. Koksbang, J. Barker, H. Shi, M.Y. Saidi, *Cathode materials for lithium rocking chair batteries*, Solid State Ionics, 84 (1996), 1-23.

[4] P.P. Prosini, M. Carewska, S. Scaccia, P. Wisniewski, S. Passerini, M. Pasqualib, *A New Synthetic Route for Preparing $LiFePO_4$ with Enhanced Electrochemical Performance*, J. Electrochem. Soc., 149 (2002), A886-A890.

[5] T. Ohzuku, A. Ueda, M. Nagayama, *Electrochemistry and Structural Chemistry of $LiNiO_2$ (R3m) for 4 Volt Secondary Lithium Cells*, J. Electrochem. Soc., 140 (1993), 1862-1870.

[6] T. Ohzuku, M. Kitagawa, T. Hirai, *Electrochemistry of Manganese Dioxide in Lithium Nonaqueous Cell*, J. Electrochem. Soc., 137 (1990), 769-775.

[7] H. Huang, S.C. Yin, L. F. Nazar, *Approaching Theoretical Capacity of $LiFePO_4$ at Room Temperature at High Rates, Electrochem. Solid-State Lett.*, 4 (2001), A170-A172.

[8] Y. Xia, T. Sakai, T. Fujieda, X.Q. Yang, X. Sun, Z.F. Ma, J. McBreen, M. Yoshio, *Correlating Capacity Fading and Structural Changes in $Li_{1+y}Mn_{2-y}O_{4-\delta}$ Spinel Cathode Materials*, J. Electrochem. Soc., 148 (2001), A723-A729.

[9] K.K. Lee, W.S. Yoon, K.B. Kim, K.Y. Lee, S.T. Hongb, *A Study on the Thermal Behavior*

of Electrochemically Delithiated $Li_{1-x}NiO_2$, J. Electrochem. Soc., 148 (2001), A716-A722.

[10] A.K. Padhi, K.S. Nanjundaswamy, J.B. Goodenough, *Phospho-olivines as Positive-Electrode Materials for Rechargeable Lithium Batteries*, J. Electrochem. Soc., 144 (1997), 1188-1193.

[11] A. Yamada, S.C. Chung, K. Hinokuma, *Optimized $LiFePO_4$ for Lithium Battery Cathodes*, J. Electrochem. Soc., 148 (2001), A224-A229.

[12] M. Takahashi, H. Ohtsuka,a K. Akuto, Y. Sakurai, *Confirmation of Long-Term Cyclability and High Thermal Stability of $LiFePO_4$ in Prismatic Lithium-Ion Cells*, J. Electrochem. Soc., 152 (2005), A899-A904.

[13] A.k. Paclhi, K.S. Nanjunclaswamy, C. Masquelier, S. Okada, J. B. Goodenoug, *Effect of Structure on the Fe^{3+}/Fe^{2+} Redox Couple in Iron Phosphates*, J. Electrochem. Soc. 144 (1997) 1609-1613.

[14] H.S. Kim, B.W. Cho, W.I. Cho, *Cycling performance of $LiFePO_4$ cathode material*, J. Power Sources, 132 (2004), 235-239.

[15] W. Zajac, J. Marzec, J. Mplenda, *The effect of aluminium on the electrical and electrochemical properties of phospho-olivine–a cathode material for Li-ion batteries*, Mater. Sci.-Poland, 24 (2006), 123-131.

[16] N. Penazzia, M. Arrabitoa, M. Pianaa, S. Bodoardoa, S. Panerob, I. Amadeib, *Mixed lithium phosphates as cathode materials for Li-Ion cells*, J. European Ceram. Soc., 24 (2004), 1381-1384.

[17] M. Takahashi, S.I. Tobishima, K. Takei, Y. Sakurai, Reaction behavior of $LiFePO_4$ as a cathode material for rechargeable lithium batteries, Solid State Ionics, 148 (2002), 283-289.

[18] A. Gonia, L. Lezamaa, A. Pujanab, M.I. Arriortuab, T. Rojoa, *Clustering of Fe^{3+} in the $Li_{1-3x}Fe_x$ $MgPO_4(0<x<0.1)$ solid solution*, Int. J. Inorg. Mater., 3 (2001), 937-942.

[19] M.R. Yang, W.H. Ke, S.H. Wu, *Preparation of $LiFePO_4$ powders by co-precipitation*, J. Power Sources, 146 (2005), 539-543.

[20] J. Chen, M. S. Whittingham, *Hydrothermal synthesis of lithium iron phosphate*, Electrochem. Commun., 8 (2006), 855-858.

[21] S.H. Wu, K.M. Hsiao, W.R. Liu, *The preparation and characterization of olivine $LiFePO_4$ by a solution method*, J. Power Sources, 146 (2005), 550-554.

[22] M.A.E. Sanchez, G.E.S. Brito, M.C.A. Fantini, G.F. Goya, J.R. Matos, *Synthesis and characterization of $LiFePO_4$ prepared by sol–gel technique*, Solid State Ionics, 177 (2006), 497-500.

[23] D. Wang, Z. Wang, X. Huang, L. Chen, *Continuous solid solutions $LiFe_{1-x}Co_xPO_4$ and its electrochemical performance*, J. Power Sources, 146 (2005) 580-583.

[24] A. Yamada, Y. Kudo, K.Y. Liu, *Reaction Mechanism of the Olivine-Type $Li_x(Mn_{0.6}Fe_{0.4})PO_4$ $(0 \leqq x \leqq 1)$*, J. Electrochem. Soc., 148 (2001), A747-A754.

[25] N.J. Yun, H.W. Ha, K.H. Jeong, H.Y. Park, K. Kim, *Synthesis and electrochemical properties of olivine-type $LiFePO_4$/C composite cathode material prepared from a poly(vinyl alcohol)-containing precursor, J. Power Sources*, 160 (2006), 1361-1368.

[26] T.H. Cho, H.T. Chung, *Synthesis of olivine-type $LiFePO_4$ by emulsion-drying method*, J. Power Sources, 133 (2004), 272-276.

[27] S. Scaccia, M. Carewska, P. Wisniewski, P.P. Prosini, *Morphological investigation of sub-micron $FePO_4$ and $LiFePO_4$ particles for rechargeable lithium batteries*, Mater. Res. Bull., 38 (2003), 1155-1163.

[28] C. M. Julien, K. Zaghib, A. Mauger, M. Massot, A. Ait-Salah, M. Selmane, F. Gendron, *Characterization of the carbon coating onto $LiFePO_4$ particles used in lithium batteries*, J. Appl. Phys. 100 (2006) 063511-1 – 063511-7.

[29] Z. Chena, J.R. Dahn, *Reducing Carbon in $LiFePO_4$/C Composite Electrodes to Maximize Specific Energy, Volumetric Energy, and Tap Density*, J. Electrochem. Soc., 149 (2002), A1184-A1189.

[30] D. Wang, H. Li, S. Shi, X. Huang, L. Chen, *Improving the rate performance of $LiFePO_4$ by Fe-site doping*, Electrochim. Acta, 50 (2005), 2955-2958.

[31] R. Dominko, M. Bele, M. Gaberscek, M. Remskar, D. Hanzel, S. Pejovnik, J. Jamnik, *Impact of the Carbon Coating Thickness on the Electrochemical Performance of $LiFePO_4$/C Composites*, J. Electrochem. Soc., 152 (2005), A607-A610.

[32] S.T. Myung, S. Komaba,, N. Hirosaki, H. Yashiro, N. Kumagai, *Emulsion drying synthesis of olivine $LiFePO_4$/C composite and its electrochemical properties as lithium intercalation material*, Electrochim. Acta, 49 (2004), 4213-4222.

[33] J.D. Wilcox, M.M. Doeff, M. Marcinek, R. Kostecki, *Factors Influencing the Quality of Carbon Coatings on $LiFePO_4$*, J. Electrochem. Soc. 154 (2007) A389-395.

[34] T. Nakamura, Y. Miwa, M. Tabuchi, Y. Yamada, *Structural and Surface Modifications of $LiFePO_4$ Olivine Particles and Their Electrochemical Properties*, J. Electrochem. Soc., 153 (2006), A1108-A1114.

[35] M.M. Doeff, Y. Hu, F. McLarnon, R. Kostecki, *Effect of Surface Carbon Structure on the Electrochemical Performance of $LiFePO_4$*, Electrochem. Solid-State Lett., 6 (2003), A207-A209.

[36] D.D. MacNeila, Z. Lub, Z. Chenb, J.R. Dahn, *A comparison of the electrode/electrolyte reaction at elevated temperatures for various*

Li-ion battery cathodes, J. Power Sources, 108 (2002), 8-14.

Primary Authors

George Ting-Kuo Fey, Chair Professor of Chemical and Materials Engineering at National Central University, Taiwan, R.O.C. He received the Ph D. degree in Inorganic Chemistry, University of Massachusetts, 1973. Recent work has been in the fields of high-voltage cathode materials, lithium mixed metal oxides, coating methods for cathode materials, and mass production of $LiFePO_4$ for high-power lithium-ion cells.